

CALIBRATION FOR THE MONTE CARLO SIMULATION OF ION IMPLANTATION IN RELAXED SIGE

Robert Wittmann, Andreas Hössinger, and Siegfried Selberherr

Institute for Microelectronics, Technische Universität Wien

Gusshausstr. 27–29, A-1040 Vienna, Austria

Abstract. SiGe-based CMOS devices have significant performance enhancements compared to pure silicon devices. We have extended our Monte Carlo ion implantation simulator for $\text{Si}_{1-x}\text{Ge}_x$ targets in order to study the formation of shallow junctions. SiGe has a larger nuclear and electronic stopping power for ion implanted dopants compared to pure silicon due to the heavier and electron-rich germanium. It turned out that the Lindhard correction parameter of the electronic stopping model can be adjusted by a linear function of the germanium content to adopt the strength of the electronic stopping. The successful calibration for the simulation of arsenic and boron implantations in $\text{Si}_{1-x}\text{Ge}_x$ is demonstrated by comparing the predicted doping profiles with SIMS measurements. Thereby the non-linear shift towards shallower profiles with increasing germanium fraction is analyzed. Finally, the simulation result of source/drain implants for a MOS-transistor structure on a SiGe substrate is presented.

INTRODUCTION

While the first transistor was developed in 1947 by using germanium as the semiconductor material and GaAs devices have demonstrated high switching speed, it is silicon which completely dominates the present semiconductor market. This development has arisen due to the low cost of silicon CMOS technology. This mainstream technology offers the feasibility to produce billions of transistors on a single wafer, all with nearly identical properties. The fabrication processes and the device performance rely heavily on a number of natural properties of silicon, for instance, the availability of a good oxide. For alternative semiconductor materials much more expensive fabrication processes must be used, whereby the phenomenal yields achievable on a silicon CMOS line cannot be reached. The increase in packing density and performance of CMOS has been achieved by downscaling transistors and circuits over the years. One drawback of silicon is its relatively small carrier mobility. Since the device speed depends on how fast the carriers can be transported through the device under sustainable low operating voltages, silicon can be regarded as a relatively slow semiconductor. One of the most promising alternatives for the replacement of bulk silicon substrates in CMOS technology are silicon-germanium (SiGe) alloys.

SiGe alloys offer the possibility of bandgap engineering, enhanced carrier mobility, and a higher dopant solubility compared to pure silicon. The remarkable potential of

the SiGe material technology arises from the possibility to modify its properties by altering the composition. For instance, the band gap decreases from 1.12 eV (pure silicon) to 0.66 eV (pure germanium) at room temperature. The band structure can also be tailored by strain. By building different kinds of Si–SiGe heterostructures various properties for device design can be optimized. An excellent example is the heterojunction bipolar transistor (HBT) which enables higher switching-speed performance compared to the conventional silicon based transistor. The HBT is now applied in high frequency applications competing with III-V technologies. Of great importance for the semiconductor industry is strained silicon CMOS technology based on relaxed SiGe, and associated with it, the heterojunction field effect transistor (HFET). Theoretical considerations predict that for a similar gate-length to CMOS technology, heterostructure CMOS technology has twice the speed and a factor of 4 to 6 lower power-delay product (1). At present, the major challenge for the SiGe technology is the defect density of available virtual substrates or bulk SiGe substrates, which is still too large to achieve economic yields. With the amount of capital and knowledge invested in silicon based devices, the pressure is enormous to continue producing silicon based devices. The CMOS compatible SiGe material system which enables higher speed performance is a way to further use existing knowledge and manufacturing infrastructure.

One of the key processes in the fabrication of state-of-the-art CMOS devices is ion implantation. Ion implantation is the primary technology to introduce doping atoms into semiconductors to form devices and integrated circuits. The reason for the application of this technology is mainly the high accuracy in adjusting the doping concentration and the uniformity of the implantation across large wafers. A subsequent thermal annealing step often only repairs the induced crystal defects while it barely redistributes the dopant atoms. Therefore the distribution of the dopants in the final device is mainly determined by the ion implantation step, whereby the channeling effect caused by the anisotropy of the crystal plays a major role. Moreover effects resulting from non planar surfaces, can significantly influence the device behavior. The ion implantation process can effectively be simulated on computers. The capability of accurately predicting doping profiles can significantly reduce integrated process development and implementation time. In particular, the ongoing trend of scaling device feature sizes down into the sub-100nm regime puts high demands on the accuracy of simulation results.

Analytical ion implantation simulation tools which are often used due to their simplicity cannot accurately predict doping profiles for complex targets, for instance, multilayer targets or advanced devices with junction depths in the range of few nanometers. For a compound target like SiGe, the range predictions will be still worse, because the doping profiles additionally depend on the germanium fraction in a non-linear manner. The alternative are physics-based Monte Carlo methods which use an atomistic approach and, therefore, are able to simulate the channeling effect or the implantation induced point defects in crystalline targets as well. The accuracy of the simulation is mainly determined by the complexity of the models that describe the physical behavior. These models are applicable for a wide range of implantation conditions without the need for an additional calibration. One drawback of the Monte Carlo method are fairly long computing times, which is the main reason why the use

of Monte Carlo simulation tools as standard ion implantation tools is usually avoided in technology optimization. However, the formation of ultra-shallow junctions by ion implantation technology is a prerequisite for the construction of sub-100nm transistors. Therefore exact knowledge of the as-implanted doping profile and of the ion implantation induced crystal damages is required in order to facilitate SiGe-based CMOS technology.

THE SIMULATOR

All Monte Carlo simulation experiments were performed with the object-oriented, multi-dimensional ion implantation simulator MCIMPL-II (2), (3). The simulator is based on a binary collision approximation (BCA) and can handle arbitrary three-dimensional device structures consisting of amorphous and crystalline materials. In order to optimize the performance, the simulator uses cells arranged on an ortho-grid to count the number of implanted ions and of generated point defects. The final concentration values are smoothed and translated from the internal ortho-grid to an unstructured grid suitable for subsequent process simulation steps like finite element simulations for annealing processes.

MONTE CARLO IMPLANTATION IN SiGe ALLOYS

Principle of the Monte Carlo Method

The Monte Carlo method is based on imitating the random behavior of ions at an atomistic level. Particularly the position where an ion hits the crystalline target is calculated using appropriately scaled random numbers. Furthermore, the lattice atoms of the target are in permanent movement due to thermal vibrations. Thus, the actual positions of the vibrating atoms in the target are also simulated with random deviations. The ion implantation process is accurately simulated by computing a large number N of individual ion trajectories through a semiconductor material. The trajectory of each implanted ion is determined by the interactions with the atoms and electrons of the target material. The incoming doping atoms are slowed down due to the nuclear and electronic stopping power of the target material. The final position of an implanted ion is reached where it has lost its kinetic energy. The Monte Carlo simulator uses an atomistic crystal model which enables to simulate the channeling effect of ions in crystalline targets. Additionally, the Kinchin-Pease model is used to calculate the vacancies and interstitials which are generated by an ion (4). Being based on random numbers, the results obtained with the Monte Carlo method are never exact, but they converge to the used model characteristics by increasing the number N of simulated ions. The statistical error vanishes for $N \rightarrow \infty$. The reduction of the statistical fluctuation of doping profiles is performed through a sophisticated smoothing algorithm based on the Bernstein polynomials (3). The main advantage

of the Monte Carlo method is that it is a physically based method and therefore it is easily extendable to new target materials with the need for only calibrating the electronic stopping model for each dopant species.

Modelling of the SiGe Crystal

Silicon and germanium, which both crystallize in the diamond lattice structure, are completely miscible forming $\text{Si}_{1-x}\text{Ge}_x$ solids with x ranging from 0 to 1. For $\text{Si}_{1-x}\text{Ge}_x$ crystals the lattice parameter $a(x)$ depends on the germanium fraction x and can be calculated according to the quadratic expression [1] with sufficient accuracy (5). Vegard's law determines the SiGe lattice parameter only by a linear interpolation of the parameters of the end-point elements Si and Ge. Whereas the relation [1] takes the known small departure from Vegard's law into account and approximates the experimental data with a maximum deviation of about 10^{-3} Å.

$$a(x) = 0.02733 x^2 + 0.1992 x + 5.431 \quad (\text{Å}) \quad [1]$$

While the ion moves through the target, a local crystal model is built up around the actual ion position for searching the next collision partner (Figure 1). The selection of the target atom species in the crystal model is defined by probability x for germanium and $1 - x$ for silicon, respectively. This random choice of the atom species is acceptable because no ordering has been observed in bulk SiGe alloy crystals and ordering mechanisms in epitaxial grown layers are still under investigation.

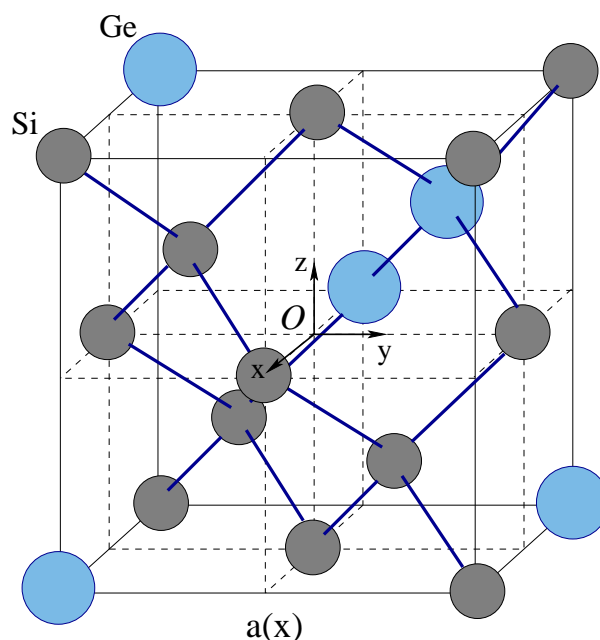


Fig. 1: $\text{Si}_{1-x}\text{Ge}_x$ crystal simulation model

The interaction of the moving ion with an atomic nucleus of the target (nuclear stopping) can be treated as an elastic collision process, whereas the interaction with the electrons can be treated as an inelastic process without any scattering effects (electronic stopping). The binary collision approximation assumes that only two particles, the ion (atomic number Z_1 , mass M_1 , energy E) and one target atom (atomic number Z_2 , mass M_2) are involved in one scattering process. While the moving particle passes and is deflected, the stationary particle recoils or at least activates thermal lattice vibrations. The final velocities and trajectories can be simply found from the conservation of energy and momentum of the system. For solving this two-body problem it is convenient to transform the scattering process from the laboratory coordinates to the center-of-mass coordinate (CM) system in which a single particle with transformed energy E_c moves in a stationary potential $V(r)$. The scattering angle Θ in the CM system is determined by [2] and depends on the energy E_c , the interatomic potential $V(r)$, and the impact parameter p (6). In [2], r_0 is the distance of minimum approach between the particles and it is determined by the real root of the denominator.

$$\Theta(p, E_c) = \pi - 2 p \int_{r_0}^{\infty} \frac{dr}{r^2 \sqrt{1 - \frac{V(r)}{E_c} - \frac{p^2}{r^2}}} \quad [2]$$

The inverse transformation leads to equation [3] which determines the scattering angle ϑ of the ion in the laboratory system.

$$\tan \vartheta = \frac{\sin \Theta}{\frac{M_1}{M_2} + \cos \Theta} \quad [3]$$

From [3] it can be derived that if the ion is heavier than the target atom ($M_1 > M_2$) then a maximal scattering angle $\vartheta_{\max} < 90^\circ$ exists according to [4].

$$\sin \vartheta_{\max} = \frac{M_2}{M_1} \quad [4]$$

An interesting conclusion can be drawn from [4] for the Monte Carlo implantation in SiGe target materials. For example, if an arsenic ion hits a silicon atom ($M_1/M_2 = 2.68$) then $\vartheta_{\max} = 22^\circ$, and if the arsenic ion hits the heavier germanium atom ($M_1/M_2 = 1.07$) then a larger maximal scattering angle $\vartheta_{\max} = 69^\circ$ is possible. Due to the fact that the angles of subsequent collisions have to be added up for a turn around from the incident direction, the backscattering probability for the dopant atoms increases with the germanium content in SiGe. Figure 2 demonstrates the shift to shallower profiles by comparing SIMS measurements of 60 keV arsenic implantations into SiGe targets with a difference in the germanium fraction of 15%. This useful property of SiGe can be exploited to reduce the vertical junction depth needed to further scale down the MOS-transistor structure in the deep sub-100nm range.

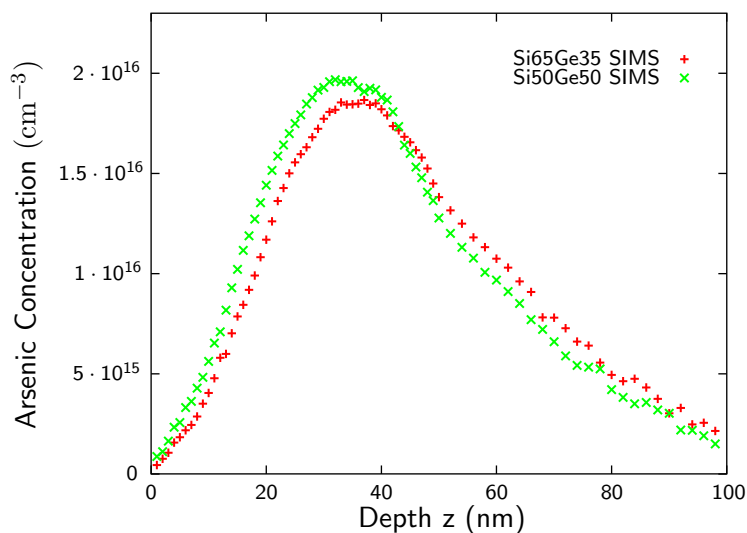


Fig. 2: SIMS comparison of 60 keV arsenic implantations in $\text{Si}_{0.65}\text{Ge}_{0.35}$ and $\text{Si}_{0.5}\text{Ge}_{0.5}$

Electronic Stopping

The total stopping process of the ions in the target solid is modeled as a sequence of alternating nuclear and electronic stopping processes. The electronic stopping process is calculated by using the Hobler model which extends the Lindhard electronic stopping model (amorphous model) to crystalline silicon (7). The only physical parameter required for this model is the impact parameter which is determined when selecting a collision partner. Due to the fact that the model implies a dependence on the charge and the mass of the atoms of the target material the electronic stopping power is averaged in the case of a compound material like SiGe. SiGe has a larger electronic stopping power than silicon, which is caused by the higher electron density of SiGe due to the electron-rich germanium atom (8). In addition to the Lindhard correction parameter k which adopts the strength of the electronic stopping, three other empirical parameters are necessary for each dopant species in crystalline silicon.

CALIBRATION

Arsenic Implantation in SiGe

We are studying the implantation of arsenic as an n-type and boron as a p-type dopant in crystalline SiGe targets with different composition. Therefore, the Monte Carlo ion implantation simulator has been extended from silicon to $\text{Si}_{1-x}\text{Ge}_x$ by calibrating the empirical electronic stopping model used to accurately simulate the electronic stopping process in crystalline silicon. For this calibration it turned out

to be most advantageous to arrange the Lindhard correction parameter k as a linear function of the germanium fraction x and let the other three parameters of the model unchanged. The equation [5] determines the parameter $k_{As}(x)$ for arsenic and it could be verified from pure silicon up to a germanium content of 50% by comparison with SIMS measurements (Figure 3).

$$k_{As}(x) = 1.132 + 1.736 x \quad [5]$$

Figure 3 shows the simulated and experimental doping profiles of arsenic implantations into $Si_{1-x}Ge_x$ layers with a thickness of 150 nm on a silicon substrate. All implantations were simulated with an energy of 60 keV, a dose of 10^{11} cm^{-2} , a tilt of 7° , and a twist of 15° . The figure demonstrates the effect of the germanium fraction in $Si_{1-x}Ge_x$ targets on profiles from arsenic implants. Two effects can be observed in this figure. Firstly, with increasing germanium fraction there is a shift towards shallower arsenic profiles. Secondly, the germanium content produces a stronger decline of the arsenic concentration with increasing penetration depth compared to silicon. It has been pointed out by the interpretation of [4] that the impact of nuclear collision is significantly changed if the incoming ion hits the germanium atom which is heavier than the silicon atom. This causes an increased backscattering probability for the dopant atoms. The larger electronic stopping power of $Si_{1-x}Ge_x$ compared to pure silicon increases with the germanium fraction x and causes a stronger decline of the concentration profiles in SiGe.

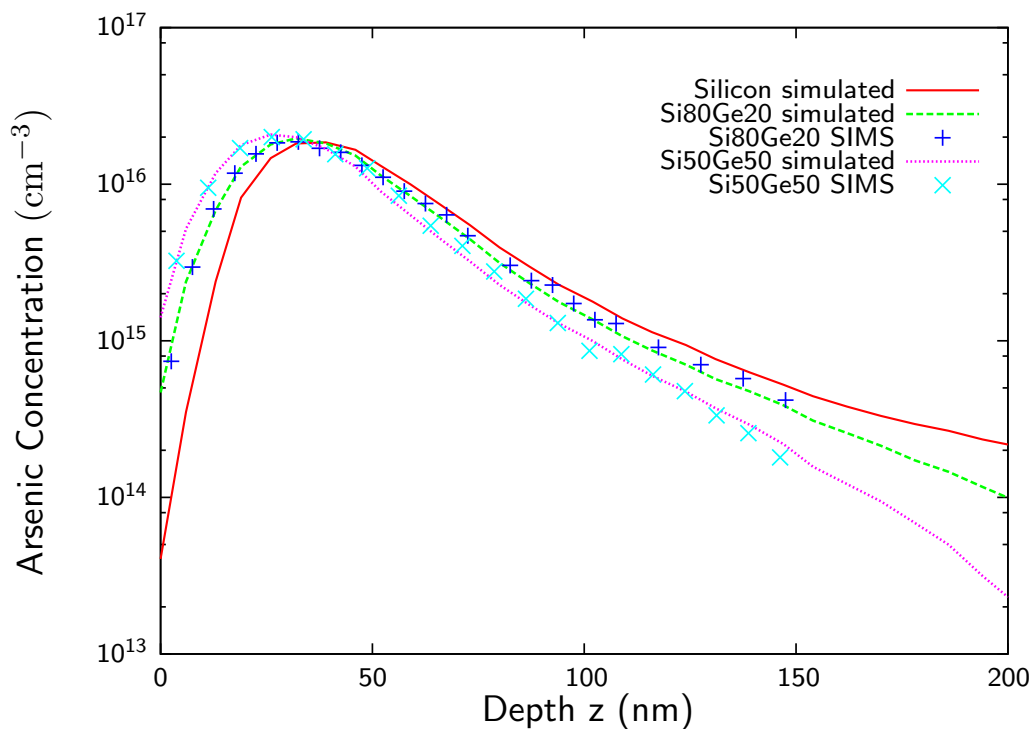


Fig. 3: Simulated 60 keV arsenic implantations in $Si_{1-x}Ge_x$ with $x = 0, 20\%, 50\%$ compared to SIMS measurements

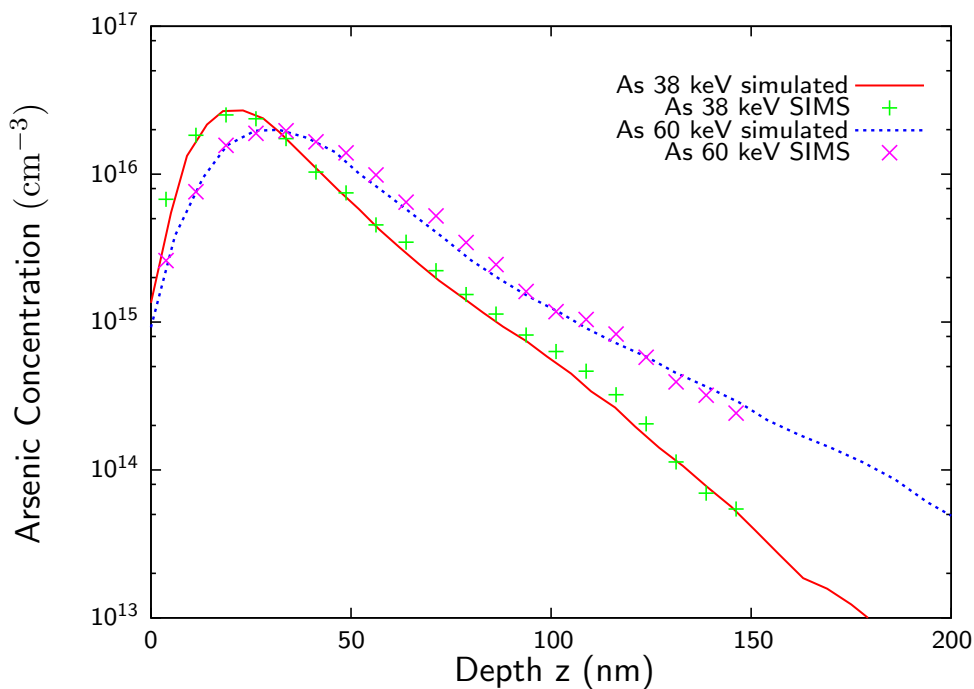


Fig. 4: Simulated 38 keV and 60 keV arsenic implantations in a $\text{Si}_{0.65}\text{Ge}_{0.35}$ target, compared to SIMS measurements

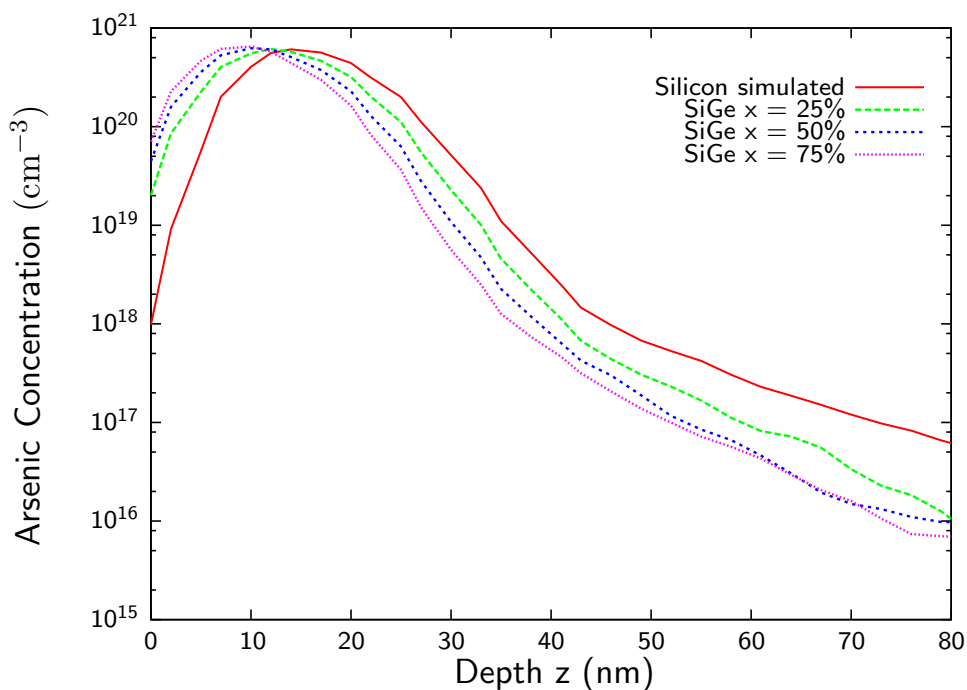


Fig. 5: Simulated 15 keV arsenic profiles in $\text{Si}_{1-x}\text{Ge}_x$ with $x = 0, 25\%, 50\%, 75\%$

Figure 4 demonstrates the successful calibration of the simulator which is valid for other energies too. It compares arsenic implants in a $\text{Si}_{0.65}\text{Ge}_{0.35}$ layer with a thickness of 150 nm performed with 38 keV and 60 keV, respectively. These profiles

were simulated with a dose of 10^{11} cm^{-2} in which the ion beam was tilted by 7° and twisted by 15° . Figure 5 presents simulated arsenic profiles performed with a lower energy and a higher dose. It again demonstrates the effect of the germanium content which facilitates the forming of shallow junctions but the trend to shallower profiles is considerably non-linear. The difference between $x = 0$ and $x = 0.25$ profiles is larger than the difference between $x = 0.5$ and $x = 0.75$ profiles, for instance. All implantations were performed with an energy of 15 keV, a dose of 10^{15} cm^{-2} , a tilt of 7° , and a twist of 22° .

Boron Implantation in SiGe

For the calibration of boron implantations in $\text{Si}_{1-x}\text{Ge}_x$ a linearly rising function for the parameter $k_B(x)$ depending on x according to [6] was used, whereas for the other three parameters of the model the values from crystalline silicon could be applied.

$$k_B(x) = 1.75 + 0.75 x \quad [6]$$

Figure 6 shows the simulated and experimental doping profiles of boron implantations into a $\text{Si}_{1-x}\text{Ge}_x$ layer with a thickness of almost 330 nm on a silicon substrate. All implantations were simulated with an energy of 50 keV, a dose of 10^{15} cm^{-2} , and a tilt of 7° . Additionally, a native oxide on the wafer surface with a layer thickness of 1 nm was taken into account for the simulation of the implantation of boron dopants.

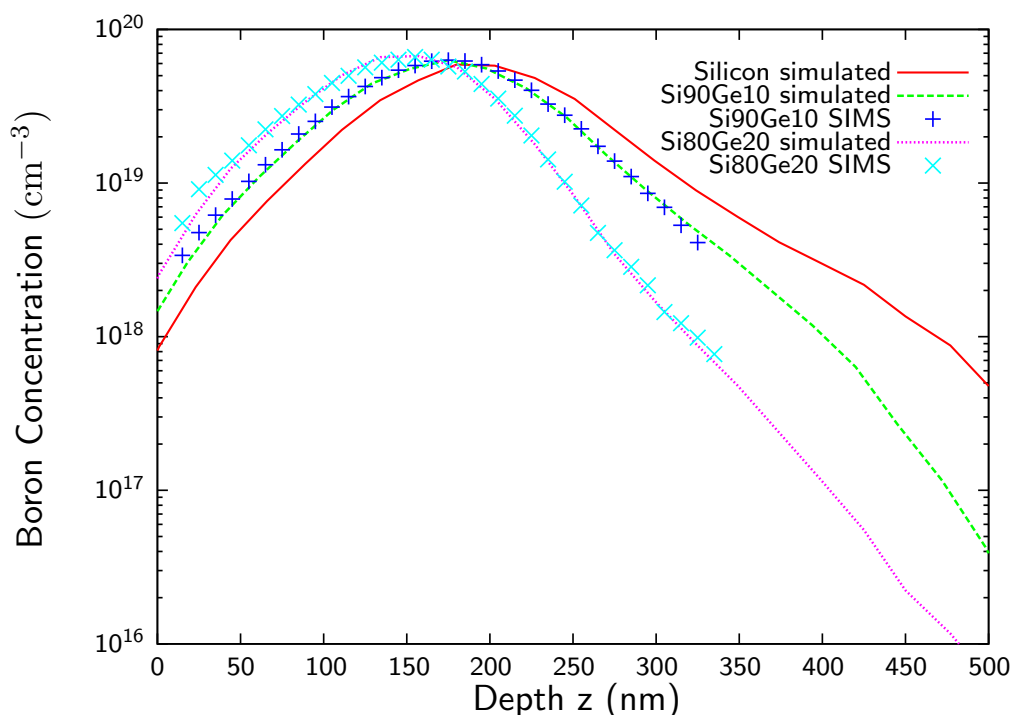


Fig. 6: Simulated 50 keV boron implantations in $\text{Si}_{1-x}\text{Ge}_x$ with $x = 0, 10\%, 20\%$ compared to SIMS measurements

Figure 6 points out that boron implants in $\text{Si}_{1-x}\text{Ge}_x$ show qualitatively the same characteristics as arsenic implants. Additionally, a larger effect of the germanium fraction for shifting the profiles towards the surface can be observed. Figure 7 compares simulated boron profiles in targets with different germanium content. All simulations were performed with an energy of 5 keV, a dose of 10^{15} cm^{-2} , and a tilt of 7° . The effect of the germanium fraction on the low-energy boron profiles is extremely non-linear.

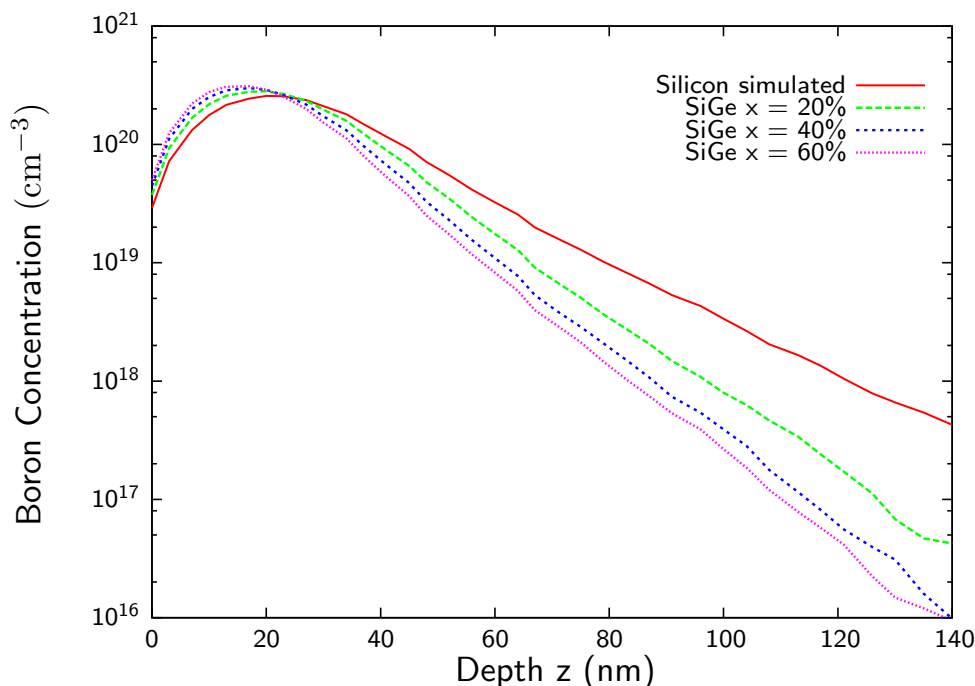


Fig. 7: Simulated 5 keV boron profiles in $\text{Si}_{1-x}\text{Ge}_x$ with $x = 0, 20\%, 40\%, 60\%$

TWO-DIMENSIONAL MOSFET APPLICATION

$\text{Si}_{1-x}\text{Ge}_x$ alloys can be applied to construct strained silicon CMOS devices. One possible MOSFET structure is the surface channel HFET in which in-plane electron mobilities approaching $3000 \text{ cm}^2/\text{Vs}$ have been reported (9). The surface channel device has a single layer of thin strained silicon (typically 10 nm), grown on top of a thick, relaxed SiGe buffer layer. The biaxial tensile strain in the strained silicon layer can be tailored by the germanium content of the relaxed SiGe layer. This structure can be used for n- or p-MOSFETs depending on the implanted dopant type in the layers. The excellent properties of $\text{Si}_{1-x}\text{Ge}_x$ alloys for forming shallow vertical junctions are demonstrated with a two-dimensional MOSFET example application. We have simulated arsenic source/drain and extension implants for a 100 nm n-MOSFET structure on a $\text{Si}_{0.75}\text{Ge}_{0.25}$ substrate. Using scaling considerations, a source/drain vertical junction depth of 40 nm to 80 nm is recommended for processing of a 100 nm gate MOS transistor. Figure 8 shows the Monte Carlo arsenic source/drain and extension

implants for such a transistor. The simulation was performed with 2.000.000 simulated ions per each implantation step. In the first implantation step the source/drain extensions were formed with an energy of 15 keV, a dose of $4 \cdot 10^{13} \text{ cm}^{-2}$, a tilt of 7° , and a twist of 22° . The source/drain implantation step was performed with an energy of 45 keV and a dose of $2 \cdot 10^{15} \text{ cm}^{-2}$. Although a relatively large energy of 45 keV was used, the required junction depth was met.

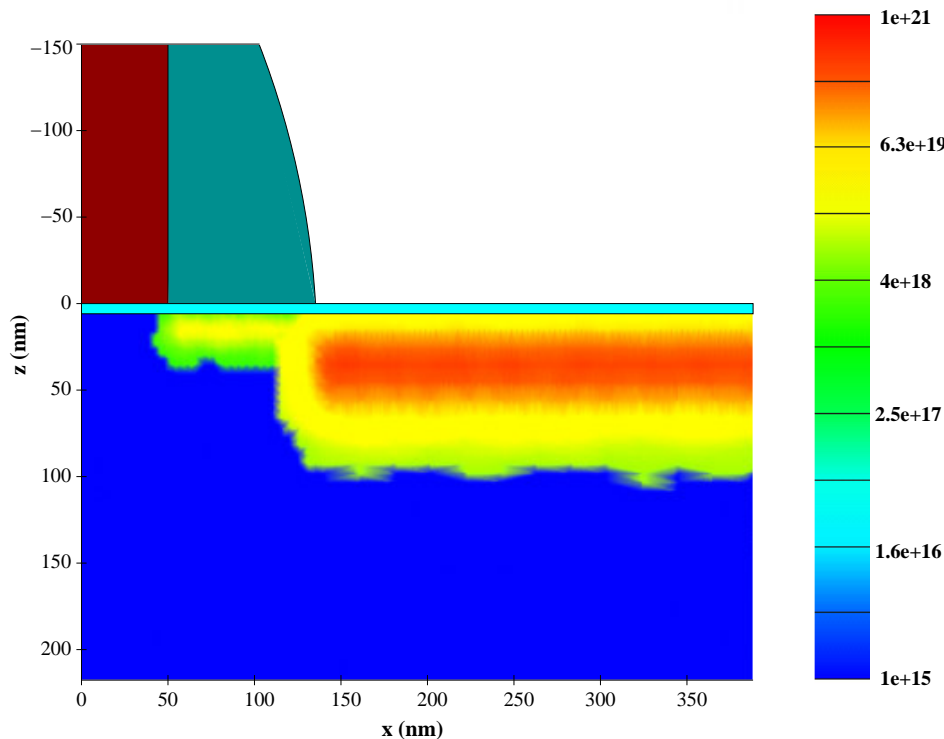


Fig. 8: Simulated cross-section of a 100 nm gate n-MOSFET structure on a relaxed $\text{Si}_{0.75}\text{Ge}_{0.25}$ substrate for SiGe-based CMOS technology

SUMMARY AND CONCLUSION

Relaxed SiGe layers strongly facilitate the forming of shallow vertical junctions which are a prerequisite to further scaling down MOSFET structures into the deep sub-100nm regime. The penetration depth for ion implanted dopant atoms in $\text{Si}_{1-x}\text{Ge}_x$ is reduced with the increase of the germanium content x at a given implantation energy. This effect arises due to the larger nuclear and electronic stopping power of the germanium atom compared to the silicon atom of the target alloy. The heavier germanium atom leads to a significantly higher backscattering probability which has been derived from the scattering integral. This integral is evaluated by the Monte Carlo simulator to determine the scattering angle of the nuclear collision process. On the other hand, the larger electronic stopping power of germanium facilitates a

stronger decline of the dopant concentration profiles. The calibration of the empirical electronic stopping model for the simulator is based on a linear relation between the Lindhard correction parameter k and the germanium fraction x for each dopant species. This assumption has been validated for arsenic and boron implantations into targets with different germanium fractions. An accurate agreement of the simulated doping profiles with the SIMS measurement data was found in all cases. Although a simple linear relation was used to include the effect of germanium on the electronic stopping power, the resulting doping profiles vary with increasing germanium fraction extremely non-linear. The inherent consideration of all involved atom species (dopant and target atoms) in the BCA approximation calculation and the existing accurate calibration for crystalline silicon has facilitated considerably the extension of the simulator MCIMPL-II to relaxed SiGe.

ACKNOWLEDGMENTS

I am indebted to Dr. Pauli Laitinen and Prof. Dr. Herbert Hutter for providing SIMS measurement data and background information about the experiments. This work has partly been supported by the Austrian Program for Advanced Research and Technology (APART) from the Austrian Academy of Science.

REFERENCES

1. D. J. Paul, *Advanced Materials*, **11**(3), 191 (1999).
2. G. Hobler and S. Selberherr, *IEEE Transactions on CAD*, **8**(5), 450 (1989).
3. R. Wittmann, A. Hössinger, and S. Selberherr, in *Proc. 15th European Simulation Symposium (ESS 2003)*, A. Verbraeck and V. Hlupic, Editors, p. 35, Delft (2003).
4. M. J. Norgett, M. T. Robinson, and I. M. Torrens, *Nuc. Eng. Des.*, **33**, 50 (1975).
5. E. Kasper and K. Lyutovich, *Properties of Silicon Germanium and SiGe:Carbon*, p. 47, Inspec, London (2000)
6. J. Ziegler, *Ion Implantation Science and Technology*, p. 207, Ion Implantation Technology Co., New York (1996).
7. G. Hobler and H. Pötzl, in *Proc. Mat. Res. Soc. Symp.*, **279**, p. 165 (1993).
8. Y. Abramov and F. Okamura, *Acta Crystallographica Section A*, **53**, p. 187 (1997).
9. C. K. Maiti, N. B. Chakrabarati, and S. K. Ray, *Strained Silicon Heterostructures: Materials and Devices*, p. 313, Institution of Electrical Engineers, London (2001)